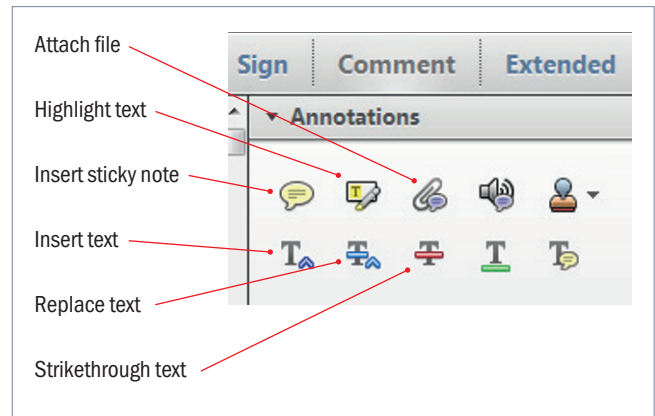


Making corrections to your proof

Please follow these instructions to mark changes or add notes to your proof. You can use Adobe Acrobat Reader (download the most recent version from <https://get.adobe.com>) or an open source PDF annotator.

For Adobe Reader, the tools you need to use are contained in **Annotations** in the **Comment** toolbar. You can also right-click on the text for several options. The most useful tools have been highlighted here. If you cannot make the desired change with the tools, please insert a sticky note describing the correction.

Please ensure all changes are visible via the 'Comments List' in the annotated PDF so that your corrections are not missed.



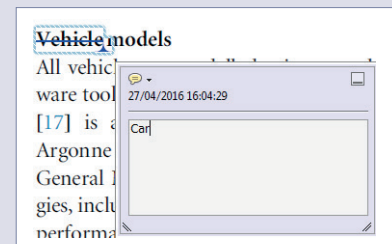
APPROVED

Do not attempt to directly edit the PDF file as changes will not be visible



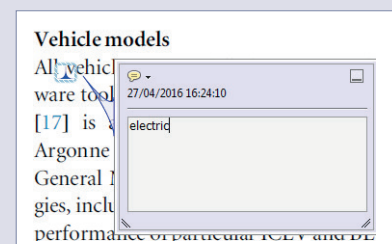
Replacing text

To replace text, highlight what you want to change then press the replace text icon, or right-click and press 'Add Note to Replace Text', then insert your text in the pop up box. Highlight the text and right click to style in bold, italic, superscript or subscript.



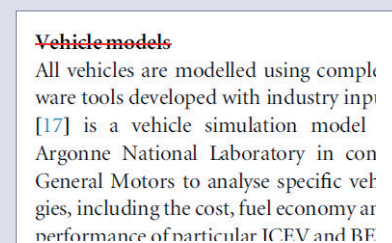
Inserting text

Place your cursor where you want to insert text, then press the insert text icon, or right-click and press 'Insert Text at Cursor', then insert your text in the pop up box. Highlight the text and right click to style in bold, italic, superscript or subscript.



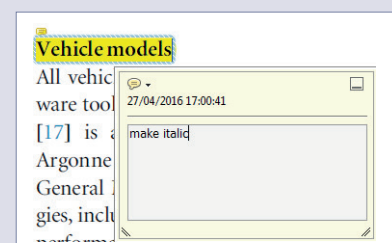
Deleting text

To delete text, highlight what you want to remove then press the strikethrough icon, or right-click and press 'Strikethrough Text'.



Highlighting text

To highlight text, with the cursor highlight the selected text then press the highlight text icon, or right-click and press 'Highlight text'. If you double click on this highlighted text you can add a comment.



QUERY FORM

JOURNAL: Laser Physics

AUTHOR: M I Ivanyan *et al*

TITLE: Mode enhancement of THz helical undulator radiation in waveguide

ARTICLE ID: abb1bd

Your article has been processed in line with the journal style. Your changes will be reviewed by the Production Editor, and any amendments that do not comply with journal style or grammatical correctness will not be applied and will not appear in the published article.

The layout of this article has not yet been finalized. Therefore this proof may contain columns that are not fully balanced/matched or overlapping text in inline equations; these issues will be resolved once the final corrections have been incorporated.

-
- Q1: Please check that the names of all authors as displayed in the proof are correct, and that all authors are linked to the correct affiliations. Please also confirm that the correct corresponding author has been indicated. Note that this is your last opportunity to review and amend this information before your article is published.
- Q2: If an explicit acknowledgment of funding is required, please ensure that it is indicated in your article. If you already have an Acknowledgments section, please check that the information there is complete and correct.
- Q3: Please be aware that the colour figures in this article will only appear in colour in the online version. If you require colour in the printed journal and have not previously arranged it, please contact the Production Editor now and refer to <https://publishingsupport.iopscience.iop.org/questions/figures-journal-articles> for pricing.
- Q4: Please check - part of this sentence is missing.
- Q5: Please check the details for any journal references that do not have a link as they may contain some incorrect information. If any journal references do not have a link, please update with correct details and supply a Crossref DOI if available.
- Q6: Please provide the volume number in reference [15].
- Q7: Please provide the page number in references [22, 23].
- Q8: Publisher location is required for book reference [33]. Please provide the missing information.

Mode enhancement of THz helical undulator radiation in waveguide

M I Ivanyan¹, A H Grigoryan¹, B K Sargsyan¹, T L Vardanyan¹, A V Tsakanian^{1,3}
and V M Tsakanov^{1,2}

¹ CANDLE Synchrotron Research Institute, Yerevan, Armenia

² Yerevan State University, 1 Alex Manoogyan, 0025, Yerevan, Armenia

E-mail: ivanian@asls.candle.am

Received 4 February 2020

Accepted for publication 19 August 2020

Published xx xx xxxx



CrossMark

Abstract

The generation of the coherent THz radiation in long undulators at the resonant wavelength is affected by the relatively broad spectrum of radiation that results in poor temporal coherence. The presence of the waveguide can essentially modify the continuous undulator radiation spectrum by converting it to a discrete one when radiation diffraction size exceeds the vacuum-chamber dimensions. In this paper the effect of a small radius circular waveguide on helical undulator radiation in the THz region is examined. It is shown that under certain conditions the presence of the waveguide can lead to radiation energy redistribution between the waveguide modes, enhancing the single resonance mode.

Keywords: helical undulator, free electron laser, waveguide

(Some figures may appear in colour only in the online journal)



1. Introduction

The development of beam-based powerful THz coherent radiation sources is a promising area of advanced accelerator physics [1–7], which opens wide research potential in the field of life and materials sciences [8]. One of the most attractive concepts for such radiation sources is the electron linear accelerator-driven self-amplified spontaneous emission (SASE) free electron laser (FEL) [9–11] or superradiant THz undulator source [12, 13], providing high radiation power by particles' coherent radiation in the undulator. Although these coherent sources are very effective, the continuous spectrum of the undulator radiation results in poor temporal coherence and a relatively broad spectrum.

One possible solution to improve the SASE FEL process is external seeding [14–16], which implies the synchronization of the FEL signal with an external signal at the same resonant wavelength, thus enhancing the resonant radiation mode and improving the brilliance of FEL output signal. The alternative approach is the so-called 'self-seeding' SASE FEL concept

[17–19], when before the radiation saturation the electron and photon beams are separated, the radiation is filtered to

Both seeding approaches result in the enhancement of the undulator resonant mode in radiation spectrum, thus improving the SASE FEL performance in UV (external seeding) or x-ray (self-seeding) wavelength range.

In the THz region, the presence of the waveguide can essentially modify the continuous undulator radiation spectrum by converting it to a discrete one, when the radiation diffraction size exceeds the vacuum-chamber dimensions. This paper is devoted to the study of the THz undulator radiation spectrum in a waveguide by means of enhancing the excited single waveguide mode.

The general approach to charged particle radiation in a perfectly conducting waveguide, using modal expansion technique, is well known and can be found for example in [20]. The radiation of the charged particle in a finite length helical undulator with a waveguide is considered in [21]. In [22], the particle radiation in a wiggler with a rectangular waveguide was studied, and the emission spectrum was compared with the free space wiggler case. The undulator radiation of electron beam in the presence of metal boundaries was analyzed in [23], where a significant difference from the free space one is shown. In [24] the coherent undulator radiation in rectangular

³ Presently at Helmholtz-Zentrum Berlin, Berlin, Germany.

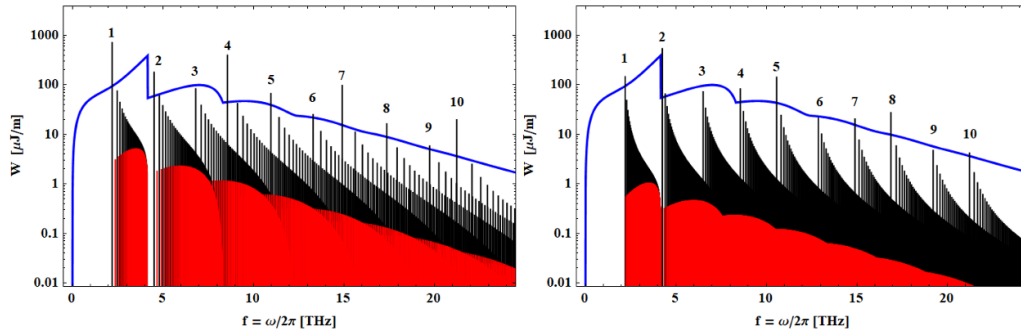


Figure 1. Discrete helical radiation spectrum for TM (red) and TE (black) modes in a waveguide and free space (blue). Waveguide radius $b = 0.1$ m (left), waveguide radius $b = 0.5$ m (right), particle energy 15 MeV, undulator parameter $K = 0.744$. The numbers indicate the index n of $TE_{n,m}$, ($n = 1, 2, 3, \dots, 10$) modes of the waveguide.

waveguide is studied in terms of the longitudinal wake function. It is shown that the radiation spectrum in a waveguide is converted to a number of sharp peaks different from the continuous radiation spectrum in free space. The peculiarities of radiation fields excited by a helically moving charge in an ideal circular waveguide under the influence of an external longitudinal magnetic field are discussed in [25]. In [26], the radiation of a charge moving along a helical trajectory inside a waveguide with dielectric filling is studied. The undulator radiation in a waveguide based on the paraxial and resonance approximations is evaluated in [27]. The impact of the waveguide walls' finite conductivity on helical radiation is studied in [28]. In [29], an explicit expression for the longitudinal wake function of the point charge helical motion in perfectly conducting pipe is given. The theoretical aspects of a waveguide THz FEL have been considered in [30]. Despite the numerous studies of undulator radiation in waveguides, the possibility of the single waveguide mode enhancement in the undulator radiation spectrum is has not been considered.

Helical undulators play an important role as a source of circular polarized electromagnetic radiation. The spectral range of this radiation may vary from THz to x-ray regions. In a THz region the spectral and spatial characteristics of undulator radiation are modified by the boundary conditions of the surrounding vacuum chamber redistributing the radiated energy among waveguide modes. As a result, the continuous energy spectrum transforms into discrete spectrum lines with sharp peaks corresponding to exited TM and TE type waveguide modes.

In this paper, the peculiarities of the THz helical undulator radiation in waveguide are studied, aiming the effective excitation of the resonant mode. The discrete spectrum in the waveguide might essentially differ from the continuous spectrum in free space, when the radiation diffraction size exceeds the vacuum-chamber dimensions. The presence of the waveguide modifies the frequency, stored energy and number of the exited modes. Depending on the waveguide radius, beam energy and undulator period, the single waveguide resonant mode in the long undulator can be enhanced. The essential part of radiated energy is then stored in the single waveguide resonant mode, producing narrowband monochromatic radiation important for

effective THz FEL performance by means of temporal coherence and radiation spectrum. In this paper, the undulator radiation in the forward direction is considered, assuming the waveguide perfectly conducts walls and neglecting resistive wakefield effects. The calculations and analyses are performed for the relativistic point charge, neglecting the space charge effects. The results are given in the rational MKSA system of units.

2. Field configurations and energy flow along waveguide

Consider the point relativistic charge q moving along the helical orbit in an infinitely long, hollow cylindrical waveguide with circular cross section of radius b and perfectly conducting walls. The charge and current densities ρ , \vec{j} for such a motion in cylindrical coordinates (r, φ, z) are given as

$$\rho = q \frac{\delta(\mathbf{r} - \mathbf{r}_0)}{r} \delta(\varphi - \omega_0 t) \delta(z - \mathbf{V}t), \quad (1)$$

$$\vec{j} = (\omega_0 r_0 \vec{e}_\varphi + V \vec{e}_z), \quad (2)$$

where $\omega_0 = 2\pi V/\lambda_u$ is the particle revolution frequency, λ_u is the undulator period, $r_0 = \lambda_u K/2\pi\gamma$ is the helix radius, $K = 0.93 B_0 [T] \cdot \lambda_u [\text{cm}]$ is the dimensionless undulator parameter, B_0 is the maximum on axis undulator magnetic field, γ is the particle Lorentz factor, V is the particle longitudinal velocity, and \vec{e}_r , \vec{e}_φ , \vec{e}_z are the corresponding unit vectors in cylindrical coordinates. The periodic magnetic field \vec{B} on the axis of the helical undulator is given by

$$\vec{B} = B_0 [\vec{e}_r \cos(k_u z - \phi) + \vec{e}_\varphi \sin(k_u z - \phi)], \quad (3)$$

with $k_u = 2\pi/\lambda_u$. An important feature of the particle motion in purely helical undulator is that the longitudinal velocity of a particle is a constant, given by

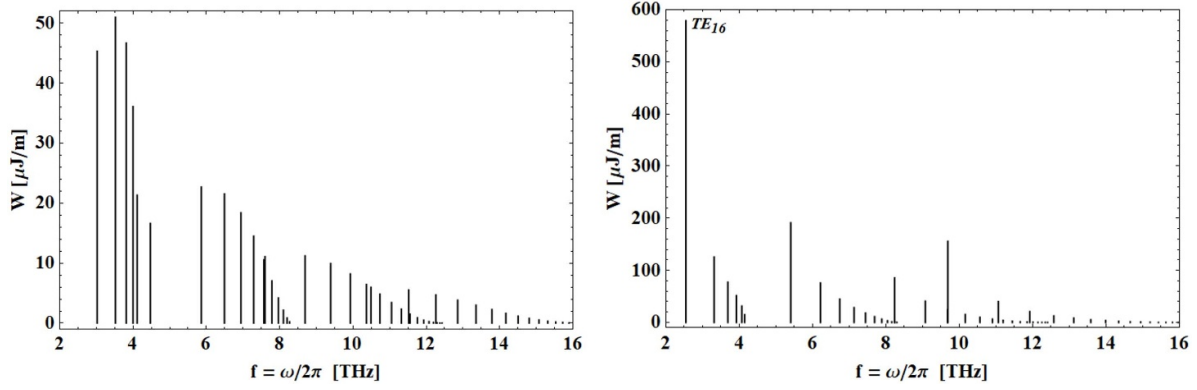


Figure 2. Discrete helical radiation spectrum for TM (left) and TE (right) modes; $b = 1$ cm, $K = 0.744$, $l_u = 8$ cm, $E = 15$ MeV. The first four sets of modes are shown: $n = 1, 2, 3$ and 4.

$$\mathbf{V} = \mathbf{c} \left\{ 1 - (1 + K^2) / 2\gamma^2 \right\}. \quad (4)$$

The radiated fields in the waveguide are defined by Maxwell's equations with the boundary conditions of vanishing the tangential component of the electric field at waveguide walls, i.e. $\mathbf{E}_z = \mathbf{E}_\varphi = 0$ at $\mathbf{r} = b$.

With the use of the modal expansion technique [31] it can be shown that the radiated fields in the waveguide are composed of both types of propagating modes: TM and TE modes. The longitudinal components of electric E_z (TM modes) and magnetic H_z (TE modes) fields in the time-space domain can be presented as

$$\mathbf{E}_z = \sum_{n,m=1}^{\infty} \mathbf{A}_{nm} \mathbf{J}_n(\alpha_{nm} \mathbf{r}/b) \exp[i(\mathbf{n}\varphi - \omega_{nm} \mathbf{t}) + \mathbf{k}_{nm} \mathbf{z}], \quad (5)$$

$$\mathbf{H}_z = \sum_{n,m=1}^{\infty} \mathbf{B}_{nm} \mathbf{J}_n(\alpha'_{nm} \mathbf{r}/b) \exp[i(\mathbf{n}\varphi - \omega'_{nm} \mathbf{t}) + \mathbf{k}'_{nm} \mathbf{z}], \quad (6)$$

with

$$\mathbf{A}_{nm} = \frac{\mathbf{q}}{2\pi\epsilon_0 b^2} \frac{\mathbf{J}_n(\alpha_{nm} \mathbf{r}_0/b)}{\mathbf{J}_n^2(\alpha_{nm})}, \quad (7)$$

$$\mathbf{B}_{nm} = \frac{\mathbf{q} \mathbf{r}_0^2 \omega_0}{2\pi b^3} \frac{i \alpha_{nm}^3}{\alpha_{nm}^2 - n^2} \frac{\mathbf{J}_n(\alpha'_{nm} \mathbf{r}_0/b)}{\mathbf{J}_n^2(\alpha'_{nm})},$$

and

$$\omega_{nm} = n\omega_0 + k_{nm}V, \quad \omega'_{nm} = n\omega_0 + k'_{nm}V,$$

$$\mathbf{k}_{nm} = \gamma_z^2 r_0^{-1} [n\beta_z \beta_\perp + f(\alpha_{nm}) \text{sign}(z - Vt)],$$

$$\mathbf{k}'_{nm} = \gamma_z^2 r_0^{-1} [n\beta_z \beta_\perp + f(\alpha'_{nm}) \text{sign}(z - Vt)],$$

$$\mathbf{f}(\mathbf{x}) = \sqrt{\mathbf{n}^2 \beta_\perp^2 - \gamma_z^{-2} \mathbf{x}^2 \mathbf{r}_0^2 / b^2}. \quad (8)$$

Here $\beta_\perp = \omega_0 \mathbf{r}_0 / \mathbf{c} = \beta_z \mathbf{K} / \gamma$ and $\beta_z = V/c$ correspond to the particle transverse and longitudinal velocities respectively, $\gamma_z = \gamma(1 + K^2)^{-1/2}$ is the particle longitudinal Lorentz factor, α_{nm} are the roots of the first-order Bessel function $J_n(\mathbf{x})$ (TM modes), α'_{nm} are the roots of $J'_n(\mathbf{x})$ (TE modes), ω_{nm} , ω'_{nm} are the excited mode frequencies, \mathbf{k}_{nm} , \mathbf{k}'_{nm} are the longitudinal wave numbers and ϵ_0 is the dielectric constant of vacuum. Note that $z - Vt > 0$ corresponds to radiated fields in front of the charge, $z - Vt < 0$ corresponds to radiated fields behind the charge, and $z - Vt = 0$ is the point charge longitudinal position. We consider the undulator radiation in the forward direction as it provides the dominant contribution to undulator radiation [32]. The transverse components for TM ($\vec{\mathbf{E}}_t^{\text{TM}}, \vec{\mathbf{H}}_t^{\text{TM}}$) and TE ($\vec{\mathbf{E}}_t^{\text{TE}}, \vec{\mathbf{H}}_t^{\text{TE}}$) modes are derived from inhomogeneous Maxwell's equations in frequency domain as [33]

$$\vec{\mathbf{E}}_t^{\text{TM}} = \frac{i \mathbf{k}_{nm} b^2}{\alpha_{nm}^2} \nabla_t \mathbf{E}_z, \quad \vec{\mathbf{H}}_t^{\text{TM}} = \epsilon_0 \frac{\omega_{nm}}{\mathbf{k}_{nm}} \vec{\mathbf{e}}_z \times \vec{\mathbf{E}}_t^{\text{TM}},$$

$$\vec{\mathbf{H}}_t^{\text{TE}} = \frac{i k'_{nm} b^2}{\alpha_{nm}^2} \nabla_t H_z, \quad \vec{\mathbf{E}}_t^{\text{TE}} = -\mu_0 \frac{\omega'_{nm}}{k'_{nm}} \vec{\mathbf{e}}_z \times \vec{\mathbf{H}}_t^{\text{TE}}, \quad (9)$$

where the transverse gradient in cylindrical coordinates is given as $\nabla_t = (\partial/\partial r, \text{in}/r)$ and μ_0 is the vacuum magnetic permeability.

The conditions for non-vanishing modes from expression under root in (8) are given by $n\gamma_z \beta_\perp \geq \alpha_{nm} \mathbf{r}_0 / b$ for TM modes and

$$n\gamma_z \beta_\perp \geq \alpha'_{nm} \mathbf{r}_0 / b \quad (10)$$

Note that the modes with index $n = 0$ are not excited in waveguide. For given n , the finite number of the modes are excited depending on particle energy and undulator parameter. The contribution of each individual mode to the radiation energy spectrum in the waveguide undulator structure is determined by the stored energy per unit length of pipe:

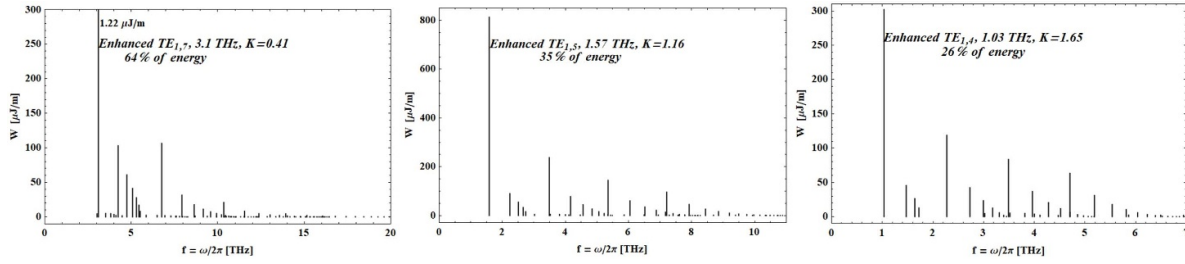


Figure 3. The waveguide undulator resonant mode enhancement for various undulator parameters: particle energy 15 MeV, waveguide radius 1 cm.

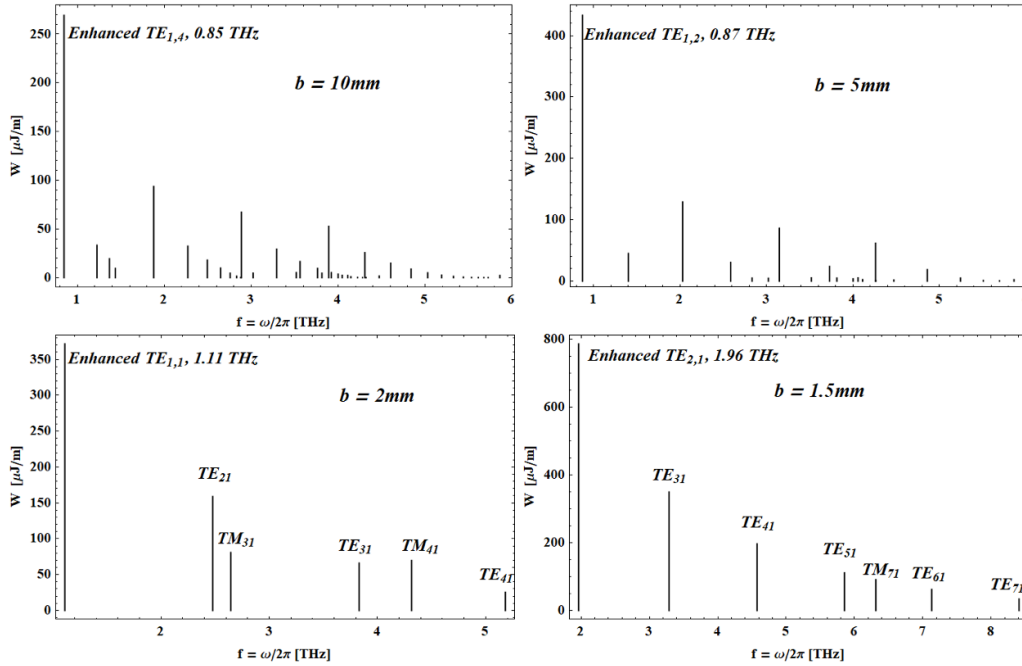


Figure 4. The waveguide undulator discrete spectrum for various radii of the waveguide.

$$W_{mn}^{TM} = \int_0^b \int_0^{2\pi} \left\{ \epsilon_0 \left| \vec{E}_{mn}^{TM} \right|^2 + \mu_0 \left| \vec{H}_{mn}^{TM} \right|^2 \right\} r dr d\varphi,$$

$$W_{mn}^{TE} = \int_0^b \int_0^{2\pi} \left\{ \epsilon_0 \left| \vec{E}_{mn}^{TE} \right|^2 + \mu_0 \left| \vec{H}_{mn}^{TE} \right|^2 \right\} r dr d\varphi. \quad (11)$$

The explicit expressions may be obtained for (11), using (5–8):

$$W_{mn}^{TM} = \frac{q^2 \omega_{nm}^2 J_n^2(\alpha_{nm} r_0 / b)}{2\pi \epsilon_0 c^2 \alpha_{nm}^2 J_n^2(\alpha_{nm})},$$

$$W_{nm}^{TE} = \frac{q^2 \omega_{nm}^2 \beta_{\perp}^2 r_0^2 J_n^2(\alpha'_{nm} a / b)}{2\pi \epsilon_0 c^2 b^2 f^2(\alpha'_{nm}) J_n^2(\alpha'_{nm}) \alpha_{nm}^2 - n^2}. \quad (12)$$

Note that an equivalent radiated energy per unit length can be obtained by calculating the radiated energy flow in waveguides through the pointing vector or the point charge energy loss per unit structure length.

3. Modal analysis

In the last decades, the development of advanced accelerator and radiation source approaches has been on the frontier of accelerator physics research. The AREAL linear accelerator (linac) project is aimed for the generation and acceleration of ultrashort electron pulses with small emittance [34]. It is based on a laser-driven RF gun and produces 0.4 ps duration electron pulses with small transverse emittance. The parameter list of the facility is presented in table 1.

After the successful operation of the 5 MeV RF photoinjector, the facility energy upgrade to 15–50 MeV is under development to run Mid-Infrared SASE FEL in a 4.5 m long undulator section with 2.7 cm period length and peak magnetic field of 0.47 T. According to GENESIS simulations, for the beam energy of 20–50 MeV an anticipated radiation power of about 50 MW at saturation length of 3.5 m is predicted in the radiation wavelength range of 2.5–15 μm [35]. In the 0.5–5 THz radiation frequency range (wavelength 60–600 μm) the second circular polarized beamline based on a helical undulator with period of 8 cm is planned for

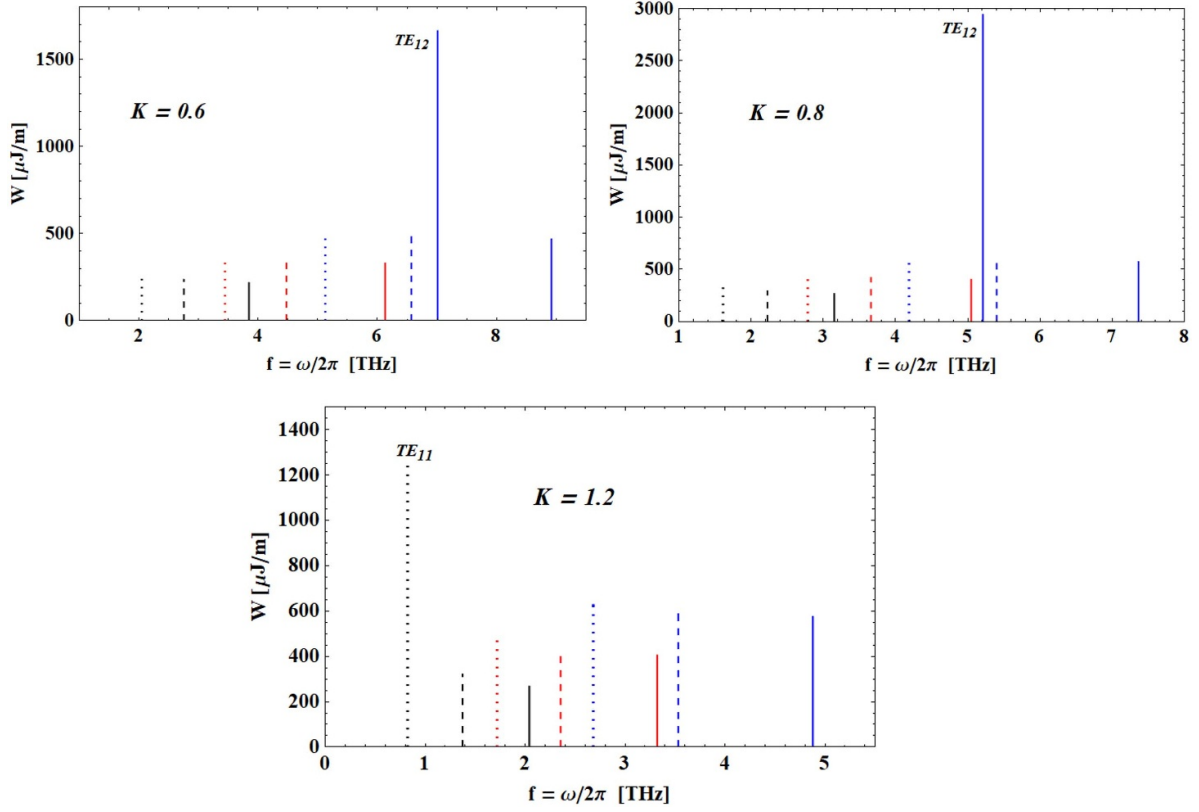


Figure 5. Undulator radiation dominant mode energy for various undulator parameters $K = 0.6, 0.8, 1.2$, particle energy $E = 12$ (black), 15 (red) and 18 (blue) MeV and undulator period $l_u = 6$ (solid), 8 (dashed) and 10 (dotted) cm.

the electron beam energy of 12–18 MeV. In this radiation wavelength range the effect of the undulator vacuum chamber (waveguide) can essentially modify the radiation spectrum. In this section, we numerically analyze the radiation spectrum dependence on the waveguide radius and the undulator parameter K considering the beam energy of 15 MeV. We are interested in the excitation of the single waveguide mode in the undulator, and therefore 10 pC point charge radiation, neglecting the space charge and beam dynamics effects, is considered. For the undulator peak magnetic field on axis of 0.1 T, the undulator parameter is $K = 0.744$, which corresponds to a helix radius of 0.32 mm with a particle revolution frequency of 3.745 GHz. The undulator radiation fundamental frequency in free space (first harmonic) is then

$$f_1 = \frac{c}{\lambda_u} \frac{2\gamma^2}{1+K^2} = 4.16 \text{ THz.}$$

In the presence of a waveguide, the continuous radiation spectrum in free space is converted to the discrete one and is composed of TM and TE waveguide propagating modes. Figure 1 presents the helical undulator radiation spectrum in free space (smooth curve) [36, 37] and the waveguide (discrete vertical lines) for a relatively large waveguide radius ($b \geq 10$ cm).

As can be seen from figure 1, for a large-radius waveguide there are many propagating modes with closed frequencies. The spectral lines of the TM modes (figure 1, red) merge,

forming an almost continuous spectrum. The TM modes' spectrum envelope in the main details repeats the spectral curve of undulator radiation in free space. For the TE modes (figure 1, black) the radiation spectrum is characterized by sharp peaks, corresponding to critical waveguide modes. The corresponding excited frequencies are given by the even number of the mode index $n = 2, 4, 6, 8$ and are adjacent to the resonant frequencies of the undulator radiation in free space. In particular, for waveguide radius $b = 0.5$ m, the first sharp peak of the mode with index $n = 2$ (figure 1, right) practically coincides with the fundamental resonant frequency $f_1 = 4.16$ THz of the free space radiation spectrum. The odd TE mode peaks correspond to the inflection point (see $n = 1$, figure 1) or local maxima (resonant frequencies, $n = 3, 5, 7$, figure 1) of the free space radiation spectrum.

As follows from (8), the waveguide excited mode frequencies are given by

$$\omega_{nm} = n\omega_0 + V\gamma_z^2 r_0^{-1} \left[n\beta_z \beta_\perp + \sqrt{n^2 \beta_\perp^2 - \gamma_z^{-2} x_{nm}^2 r_0^2 / b^2} \right], \quad (13)$$

where $\mathbf{x}_{nm} = \alpha_{nm}$ for TM modes, and $\mathbf{x}_{nm} = \alpha'_{nm}$ for TE modes. Thus for the given index \mathbf{n} , the number of propagating modes in waveguide for large $\gamma > 10$ is limited by the following condition:

$$\mathbf{x}_{nm} \leq \frac{2\pi n \gamma}{\sqrt{1+K^2}} \frac{b}{\lambda_u}. \quad (14)$$

Table 1. AREAL beam and undulator parameters.

Energy (MeV)	5–50
Bunch charge (pC)	10–200
Bunch duration FWHM (ps)	0.4–9
Norm. emittance (mm mrad)	<0.5
RMS energy spread	<0.15%
Planar undulator period (cm)	2.7
Magnetic field (T)	0.47
Helical undulator period	8 cm
Magnetic field (T)	0.1/0.25

The excited modes start from the index $n = 1$ and according to (13), the lowest frequency in radiation spectrum is given by the largest index m that satisfies an inequality (14).

Figure 2 presents the discrete radiation spectrum for TM and TE modes per unit length excited in the helical undulator anticipated for the AREAL linac THz FEL beamline. As noted above, a finite number of propagating modes correspond to each fixed index n . Each field index n produces a finite set of frequencies on the radiation spectrum distribution as shown in figure 2.

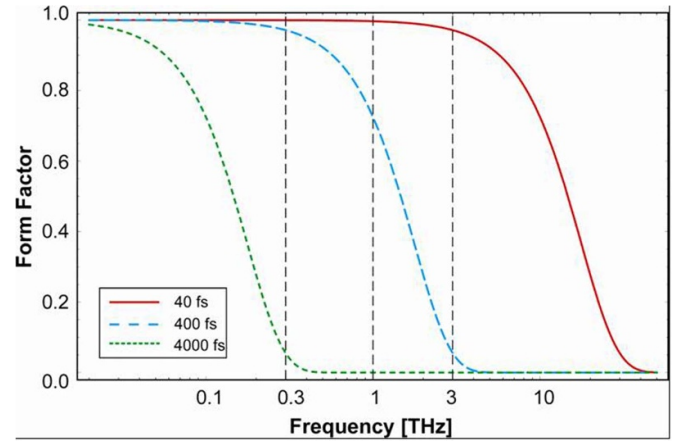
The total radiated energy per meter is about 0.45 mJ ($\sim 17.1\%$) for TM modes and 2.16 mJ ($\sim 82.9\%$) for TE modes. The radiated energy stored in TE modes is dominating. The $TE_{1,6}$ mode, excited at frequency of 2.54 THz, has the maximum energy of 0.58 mJ m^{-1} or 22.1% of the total radiated energy. This mode has a maximum index $m = 6$ for a fixed $n = 1$. The TM_{1m} and TE_{1m} excited modes frequencies and deposited energy are presented in table 2.

The shape of the radiation spectrum depends also on undulator parameter K . Figure 3 presents the radiation spectrum for various K values. As can be seen from the figure, the mode with the critical (maximal) value of the index m at $n = 1$ makes the most significant contribution to the radiation. Its contribution is especially large for a low undulator parameter K . An undulator radiation resonant frequency is high for the smaller K parameter, and according to (12) the stored radiation energy in corresponding waveguide mode is higher. For undulator parameters $K = 0.41, 1.16, 1.65$ the energy deposited in the first excited $TE_{1,7}, TE_{1,5}$ and $TE_{1,4}$ critical modes is 64%, 35% and 26% respectively. The percentage is related to the energy stored in a single waveguide mode with respect to the total radiated energy per unit length in the forward direction.

Let us consider the TE modes. The condition of non-vanishing TE modes (10) can be expressed as follows:

$$n \geq \frac{\alpha'_{nm} \lambda_u}{2\pi\gamma b} \sqrt{1 + K^2}. \quad (15)$$

We are interested only in propagating waves, so the modes with the zero first indexes can be neglected. For fixed $n \geq 1$ the eigenvalues α'_{nm} increase with increasing the m . So the number of propagating modes depends on the beam energy γ , undulator period λ_u and waveguide radius b . The analysis

**Figure 6.** The form factor for different bunch durations.

of condition (15) shows that for fixed index n , the number of propagating modes in the waveguide is limited. This number increases with the increase of n and decreases with the reduction of the waveguide radius.

The charge discrete undulator radiation spectrums in a waveguide with various radii are shown in figure 4. The undulator parameter K is taken as 1.86, which corresponds to a magnetic field of 0.25 T and undulator period of 8 cm. The particle energy is taken as 15 MeV. Here, the number of excited TE modes for $n = 1$ is equal to 4 for waveguide radius $b = 10 \text{ mm}$ and it decreases to a single TE_{11} mode, radiated at frequency of 1.1 THz, for the waveguide radius $b = 2 \text{ mm}$. The same holds for higher mode indexes ($n = 2, 3, 4$). For waveguide radius $b = 1.5 \text{ mm}$ the excited modes are started with TE_{21} mode.

As follows from the radiated field presentations, for the given waveguide radius the dominant mode, frequency and the stored energy depends on the particle energy E , undulator parameter K and period λ_u . Figure 5 presents the stored energy of undulator radiation and frequency of the dominant mode in a waveguide with a radius of 2 mm for undulator parameter $K = 0.6, 0.8, 1.2$, particle energy $E = 12, 15, 18 \text{ MeV}$ and period $\lambda_u = 6, 8, 10 \text{ cm}$. As is seen for the low undulator parameters $K = 0.6, 0.8$ and the period length of 6 cm, the maximum radiated energy is stored in TE_{12} mode at high frequency, while for the larger undulator parameter $K = 1.2$ and period $\lambda_u = 10 \text{ cm}$, the maximum radiated energy is stored in TE_{11} mode at low frequency. In all other cases, indicated in figure 5, the dominant modes are TE_{11} type with relatively lower stored energy.

So far, we considered the point charge model for the bunch. The radiation intensity for the bunch longitudinal distribution is given as [32, 38]

$$W_b(\omega) = N_e W(\omega) \{1 + (N_e - 1) g(\omega, \sigma)\}, \quad (16)$$

where $W(\omega)$ is the radiation spectrum of a single electron, N_e is the number of electrons in the bunch, $g(\omega, \sigma)$ is the bunch form factor, ω is the radiation angular frequency and σ is the

Table 2. Frequency and stored energy of TM_{1m} and TE_{1m} excited modes.

Mode index m	TM_{1m}		TE_{1m}	
	Frequency (THz)	Energy ($\mu\text{J m}^{-1}$)	Frequency (THz)	Energy ($\mu\text{J m}^{-1}$)
1	4.11	21	4.15	15
2	4.00	36	4.07	31
3	3.81	47	3.92	51
4	3.52	51	3.69	77
5	3.02	45	3.31	125
6	–	–	2.54	578

electron bunch rms duration. For the Gaussian longitudinal shape of the bunch, the form factor is expressed as χ . The form factors for Gaussian-shaped bunches with 40 fs, 400 fs and 4000 fs FWHM duration τ are shown in figure 6. Note that $\tau = 2.355\sigma$ and the frequency on the plot is in THz. As can be seen from the plot, for an electron bunch duration of 40 fs (FWHM), the emission is practically fully superradiant in the frequency range up to 3 THz. For a 400 fs bunch, the coherent radiation dominated up to frequencies of 0.5 THz. In the current design of the AREAL linac the shortest electron bunch length is 400 fs, while with the new laser pulse compression system it is anticipated to reach an electron bunch length of below 100 fs.

4. Summary

The small radius waveguide effects on THz helical undulator radiation are studied. The continuous spectrum of undulator radiation in free space is converted to a discrete one. When the radiation diffraction size exceeds the vacuum-chamber dimensions, the spectrum in the waveguide essentially differs from the continuous spectrum in free space. The presence of the waveguide modifies the frequency, stored energy and number of the excited modes. It is shown that depending on the waveguide radius, beam energy and undulator period, the single waveguide resonant mode in long undulator can be enhanced. The essential part of the radiated energy is then stored in the single waveguide resonant mode, producing narrowband monochromatic radiation. The numerical calculations show the importance of the waveguide effects for the undulator radiation performance by means of dominant mode frequency, stored energy and radiation spectrum, as well as for the generation of powerful monochromatic THz coherent radiation. For practical applications, the transition effects should be taken into account to evaluate the radiated fields in the time domain and in the formation of the discrete spectrum in a waveguide.

Acknowledgments

This work was supported by the RA MES Science Committee, in the framework of the research project No. 18T-1C144.

References

- [1] Berryman K W, Crosson E R, Ricci K N and Smith T I 1996 *Nucl. Instrum. Methods Phys. Res. A* **375** 526
- [2] van der Meer A F G 2004 *Nucl. Instrum. Methods Phys. Res. A* **528** 8
- [3] Prazeres R, Glotin F and Ortega J M 2004 *Nucl. Instrum. Methods. A* **528** 83
- [4] Gallerano G P et al 2004 *Proc. 2004 FEL2004 (Trieste, Italy)* pp 216–221
- [5] Su X, Wang D, Tian Q, Liang Y, Niu L, Yan L, Du Y, Huang W and Tang C 2018 *JINST* **13** C01020
- [6] Krainara S 2019 *Rev. Sci. Instrum.* **90** 103307
- [7] Lemery F et al 2019 *Proc. of FEL 2019 (Hamburg, Germany)* pp 688–691
- [8] Dhillon S S et al 2017 The 2017 terahertz science and technology roadmap *J. Phys. D: Appl. Phys.* **50** 043001
- [9] Schmusser P, Dohlus M and Rossbach J 2009 *Ultraviolet and Soft X-ray Free-Electron Lasers* (Berlin: Springer-Verlag) pp 207
- [10] Huang Z and Kim K-J 2007 *Phys. Rev. Spec. Top. Accel. Beams* **10** 034801
- [11] Boonpornprasert P, Krasilnikov M and Stephan F 2017 *Proc FEL2017 (Santa Fe, NM, USA)* pp 411–3
- [12] Tanikawa T, Karabekyan S, Kovalev S, Casalbuoni S, Asgekar V, Serkez S, Geloni G and Gensch M 2019 *JINST* **14** P05024
- [13] Musumeci P et al 2019 *Proc. of FEL 2019 (Hamburg, Germany)* pp 127–30
- [14] Saldin E L, Schneidmiller E A and Yurkov M V 2008 *Opt. Commun.* **281** 1179
- [15] Lambert G et al 2008 *Nat. Phys.* **296**
- [16] Gianessi L et al 2008 *Nucl. Instrum. Methods Phys. Res. A* **594** 132
- [17] Feldhaus J, Saldin E L, Schneider J R, Schneidmiller E A and Yurkov M V 1997 *Opt. Commun.* **140** 341
- [18] Geloni G, Kocharyan V and Saldin E 2011 *J. Mod. Opt.* **58** 1391
- [19] Amann J et al 2012 *Nat. Photon.* **6** 693
- [20] Motz H and Nakamura M 1959 *Ann. Phys.* **7** 84
- [21] Karapetian G G 1977 *Izv. Akad. Nauk Arm. SSR Fiz.* **12** 186–90
- [22] Haus H A and Islam N 1983 *J. Appl. Phys.* **54**
- [23] Amir A, Boscolo I and Elias L R 1985 *Phys. Rev. A* **32**
- [24] Chin Y H 1990 Coherent radiation in an undulator, LBL-29981
- [25] Dokuchaev V P 2001 *Izv. VUZov Radiofiz.* **44** 587–91
- [26] Kotanjyan A S and Saharyan A A 2007 *J. Phys. A* **40** 10641–56
- [27] Geloni G, Saldin E, Schneidmiller E and Yurkov M 2008 *Nucl. Instrum. Methods Phys. Res. A* **584** 219
- [28] Vardanyan T et al 2014 *FEL2014 Conf. (Basel, Switzerland)* pp 26–28

Q5

Q6

Q7

- [29] Ivanyan M, Tsakanian A and Vardanyan T 2015 *Armen. J. Phys.* **8** 56–64
- [30] Shobuda Y and Chin Y H 2016 *Phys. Rev. Accel. Beams* **19** 094201
- [31] Collin R E 1960 *Field Theory of Guided Waves* (New York: McGraw-Hill)
- [32] Wiedemann H 2003 *Synchrotron Radiation* (Berlin: Springer) pp 274
- [33] Jackson J D 1998 *Classical Electrodynamics* 3rd edn (Wiley & Sons)
- [34] Tsakanov V et al 2016 *Nucl. Instrum. Methods Phys. Res. A* **829** 284
- [35] Sahakyan V V et al 2018 *Arm. J. Phys.* **11** 111–6
- [36] Kincaid B M 1977 *J. App. Phys.* **48** 2684
- [37] Scheppard J C 2002 LCC-0095, SLAC (July)
- [38] Schwinger J 1949 *Phys. Rev.* **75** 1912 

Q8